Cardiovascular Modelling and Identification in Septic Shock - Experimental validation ⋆

Thomas Desaive [*], **Bernard Lambermont** [**], **Alexandre Ghuysen** [**], **Philippe Kolh** [**], **Pierre C. Dauby** [*], **Christina Starfinger** [***], **Christopher E. Hann** [***], **J. Geoffrey Chase** [***], **Geoffrey M. Shaw** [****]

[*] *Institute of Physics, University of Liège, Belgium.*
[**] *Hemodynamics Research Laboratory, University of Liège, Belgium.*
[***] *Centre of Bioengineering, University of Canterbury, Christchurch, New Zealand.*
[****] *Department of Intensive Care Medicine, Christchurch Hospital, Christchurch, New Zealand.*

Abstract:
Cardiovascular disturbances are difficult to diagnose and treat because of the large range of possible underlying dysfunctions combined with regulatory reflex mechanisms that can result in conflicting clinical data. A cardiovascular system (CVS) model and patient specific parameter identification method could better aggregate the clinical data into a more direct and simpler form for clinicians. A previously developed model and parameter identification method is improved to accurately capture physiological response to septic shock under continuous hemofiltration, further confirming the potential for using this model-based approach in critical care. Clinical data is matched with mean absolute errors less than 8% and the optimized parameters closely follow a previous study using significantly more invasive procedures and measurements.

1. INTRODUCTION

Sepsis is a most complex and serious systemic response to infection and has been shown to account for as many deaths in the USA as out-of-hospitals cardiac arrests and four times the number of those who die of breast cancer [Angus and Crowther, 2003]. More specifically, mortality rates have ranged from 25% to 80% over the last few decades [Angus et al., 2001], making septic shock and multiple organ failure one of the leading causes for morbidity and mortality in the critical care setting.

Continuous hemofiltration (HF) is a new form of renal replacement therapy which has been shown in extensive experimental studies to improve hemodynamics and survival in septic shock patients. However like most cardiac treatments the response of patients can vary considerably as well as during a single patient stay in an Intensive Care Unit (ICU).

The goal of this research is to develop a patient specific model-based approach to diagnosis and therapy in critical care using common measurements. The concept is to trial and test therapies in simulation first before intervention on patients. Clinically, this concept would be implemented either in real-time, or by improved protocols that would be developed ofline. See for example [Hann et al., 2005] for analogous model-based therapeutics approach to glucose control.

⋆ This work was supported in part by the FNRS (Belgium), Science and Technology (FRST), the University of Liège (Crédit d'Impulsion I-03/21) and the University of Canterbury (UoC Targeted Scholarship Scheme).

This research builds on a previously described cardiovascular system (CVS) model and identification process [Hann et al., 2006, Starfinger et al., 2007] to analyze and identify data, obtained from a porcine experiment of induced endotoxic shock, combined with continuous veno-venous hemofiltration (CVVH). Measurements used to identify the model parameters are the minimum and maximum volumes in the ventricles (V_{lv}, V_{rv}), pressures in aorta, pulmonary artery (P_{ao}, P_{pa}) and heart rate (HR). Every 30 minutes into the experiment new parameters are identified, uniquely representing the pig's hemodynamic condition. It is shown that the model is able to capture all the pressures and volumes when compared to measured clinical data. Furthermore, the model parameters produce similar results in the analysis of RV-vascular coupling as published earlier [Lambermont et al., 2006]. The approach of [Lambermont et al., 2006] however is significantly invasive, using a rapid vena cava constriction maneuver. This experimental validation of the model and methods shows the potential for guiding diagnosis and therapy in the ICU.

2. METHODOLOGY

2.1 CVS model

The CVS model is a lumped parameter model which was previously developed by [Smith, 2004] and is based on earlier work of [Chung et al., 1997, Olansen et al., 2000]. The original model consists of six elastic chambers, with two chambers for the left and right ventricle, respectively. These pressure- volume chambers are each characterized

by the flow in and out of the chamber, the pressure up- and downstream, the resistances of the heart valves, and inertia of the blood.

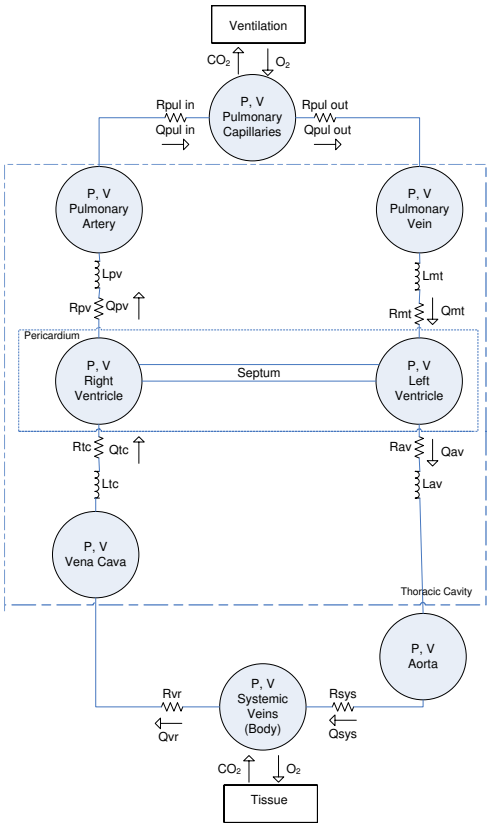

Fig. 1. Extended CVS model overview which includes additional compartments P, V_{sys} and P, V_{cap} to differentiate the arterial and venous sides of the pulmonary and systemic circulation.

The original model has been extended and an overview of the new, extended model is given in Figure 1. The extended CVS model consists of two new compartments (P, V_{sys}) and (P, V_{cap}) which represent the systemic and pulmonary capillaries, respectively. Furthermore, two new resistances, the resistance to venous return (R_{vr}) and the outflow pulmonary resistance (R_{pulout}) were added. These modifications became necessary to allow a more realistic representation of the physiological behavior as encountered during mechanical or spontaneous breathing. Note that to correctly represent the anatomy,the vena cava is now also part of the thoracic cavity, where the aorta and pulmonary capillaries are not.

2.2 Integral-Based Parameter Identification

The parameter identification method used in this research has been shown to rapidly and accurately identify virtually the entire parameter set in the presence of significant measurement noise [Hann et al., 2006, Starfinger et al., 2007] and has been successfully tested on a pulmonary embolism experiments [Starfinger et al., 2007]. This research further develops these methods.

Extended integral-based identification The main adjustments keep the arterial elastances and the pulmonary/systemic resistances fixed, allowing other parameters to be more easily and accurately calculated. Arterial compliance is defined as the change in volume $(\triangle V)$ following a change in pressure $(\triangle P)$. Arterial elastance is given as the reciprocal of the compliance. Many researchers have concluded, that arterial elastance can consequently be calculated by substituting the pulse pressure (PP) for $\triangle P$ and stroke volume (SV) for $\triangle V$ as given by the following equations [Chemla et al., 1998, Zhu et al., 1995]:

$$E_{ao} = \frac{PP_{ao}}{SV} \tag{1}$$

$$E_{pa} = \frac{PP_{pa}}{SV} \tag{2}$$

Hence, E_{ao} and E_{pa} are not identified anymore, but are directly given by the measured arterial and pulmonary artery pulse pressure (PP_{ao}, PP_{pa}) and stroke volume. Note, that even if P_{pa} should not be measured, than at least E_{ao} is given as it can be assumed that at least always P_{ao} and SV are measured signals. In this research, Equations 1 and 2 are adjusted by a multiplying factor of 1.15 as during the research, it was found that adding this factor improves the estimate for E_{ao} and E_{pa}, whereas otherwise both elastances would have been slightly underestimated. Consequently, systemic vascular resistance and elastance (R_{sys}, E_{sys}) and pulmonary vascular resistance and elastance $(R_{pulin}$ and $E_{cap})$ can now directly be calculated as follows:

$$R_{sys} = \frac{E_{ao} \cdot (\int P_{sys} - \int P_{ao})}{(P_{ao} - P_{ao0} - \int Q_{av} \cdot E_{ao})} \tag{3}$$

$$E_{sys} = \frac{\int P_{ao} - R_{sys} \cdot (\int Q_{av} - 1/E_{ao} \cdot (P_{ao} - P_{ao0}))}{\int V_{sys}} \tag{4}$$

$$R_{pulin} = \frac{E_{pa} \cdot (\int P_{cap} - \int P_{pa})}{(P_{pa} - P_{pa0} - \int Q_{pv} \cdot E_{pa})} \tag{5}$$

$$E_{cap} = \frac{\int P_{pa} - R_{pulin} \cdot (\int Q_{pv} - 1/E_{pa} \cdot (P_{pa} - P_{pa0}))}{\int V_{cap}} \tag{6}$$

Note that for reasons of clarity, the differential dt and the upper and lower limits of the integration symbol $\int$ are omitted. Usually and if not stated otherwise, the integration is done over at least one heart beat. In cases where matrices are constructed separately for ejection (systole) and filling (diastole) periods, the integrals are only calculated during these periods. More detailed information about the identification process can be found in [Hann et al., 2006, Starfinger et al., 2007].

Scaling process The complete identification process has previously been described [Starfinger et al., 2007], in this paper only a brief overview is given. To enable the calculation of integrals, waveforms are artificially generated by scaling a set of previously calculated model outputs to best fit the maximum and minimum measured data values for the pressures and volumes. The estimated signals between the discrete data points are thus forced to have

similar dynamics to model, hence minimizing modelling error. These scaled signals are then re-identified and a new CVS forward simulation is performed with the previously identified parameters producing a much closer match to the clinical data than the first initial parameter set. The simulated output is then compared to the clinical data. Subsequently, the output signals are re-scaled and new parameters are identified which are then again used to run another simulation. This iterative process is stopped when the relative error between model output and clinical data reaches a set tolerance. Figure 2 gives an overview of the overall identification process.

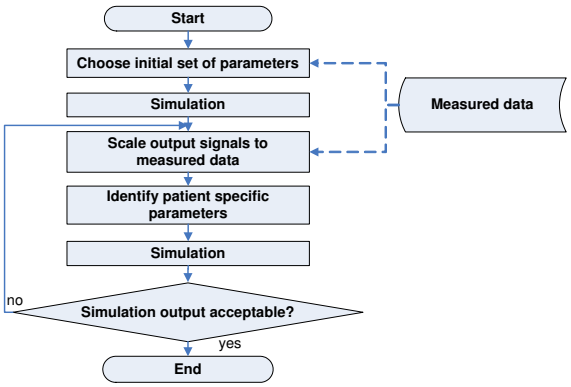

Fig. 2. Parameter identification algorithm: 1.) a set of parameters is used for an initial simulation, 2.) data is then scaled to match the measured data and 3.) identified. This process is iterated until the simulation output is acceptable.

Substitution of flow integrals during the scaling process In Equations (3) - (6) the flow integrals are not usually measured where the volumes are at least estimated. Therefore an important part of the identification process is to compute the flow integrals from the estimated or measured volumes. This calculation is easily done as follows:

$$V_{lv}(ef) - V_{lv}(eb) = -\int_{eb}^{t} Q_{av}\,\mathrm{d}t,\ eb \le t \le ef \quad (7)$$

$$V_{lv}(ff) - V_{lv}(fb) = \int_{fb}^{t} Q_{mt}\,\mathrm{d}t,\ fb \le t \le ff \quad (8)$$

$$V_{rv}(ef2) - V_{rv}(eb2) = -\int_{eb2}^{t} Q_{pv}\,\mathrm{d}t,\ eb2 \le t \le ef2 \quad (9)$$

$$V_{rv}(ff2) - V_{rv}(fb2) = \int_{fb2}^{t} Q_{tc}\,\mathrm{d}t,\ fb2 \le t \le ff2 \quad (10)$$

with eb,$eb2 \equiv$ ejection begin for LV,RV; ef,$ef2 \equiv$ ejection finish for LV,RV; fb,$fb2 \equiv$ filling begin for LV,RV and ff,$ff2 \equiv$ filling finish for LV,RV. Figure 3 shows in the upper panel the flow integral and corresponding volume signal for Q_{av}. The lower panel shows the difference between both signals which is negligible and is a result of numerical error in calculating the area under the flow graph.

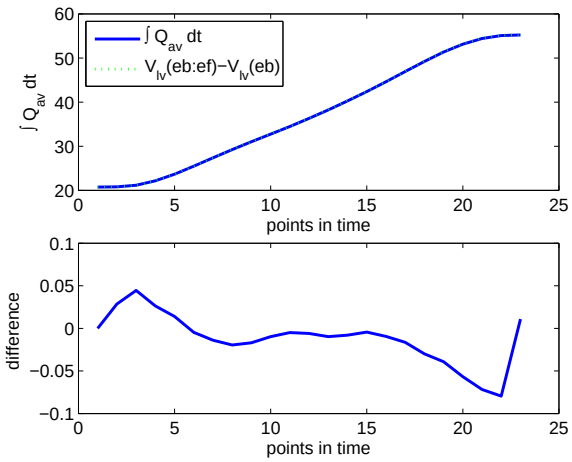

Fig. 3. Substitution of flow signal with volume signal during identification process (upper panel) and difference between these two signals (lower panel).

2.3 Experimental protocol

All experimental procedures for this experiment were reviewed and approved by the Ethics Committee of the Medical Faculty of the University of Liège. The experiments were performed on 7 healthy pigs weighing 25-30 kg, data of 6 pigs was analyzed and identified for this research. The animals were premedicated and anesthetized as described previously [Lambermont et al., 2003]. Measurements were obtained for systemic arterial pressure (P_{ao}), pulmonary arterial pressure (P_{pa}), left and right ventricle pressure and volume (P_{lv}, V_{lv}, P_{rv}, V_{rv}) as described in [Lambermont et al., 2003].

After a 30 min stabilization period, the animals received a 0.5 mg/kg endotoxin infusion (lipopolysaccharide from Escheria coli serotype 0127:B8; Sigma Chemical, St. Louis, MO, USA) over a 30 min period (T000 - T030). From 60 minutes (T060) into the experiment onwards, the animals underwent a zero-balance CVVH at a rate of 45 ml/kg/h. A $0.7m^2$ large-pore ($78\mathring{A}$) membrane with a cutoff of 80 kDa (Sureflux FH 70, Nipro, Osaka, Japan) and a Baxter BM 25- BM 14 hemofiltration device (Baxter Health Care, Munich, Germany) were used. Ultrafiltrate was replaced in the postdilution mode by a bicarbonate-buffered hemofiltration fluid (Na^+: 150mM; K^+: 3mM; bicarbonate: 30mM) at a temperature of $37°C$.

3. RESULTS

3.1 Identification of endotoxic shock

Figure 4 shows the clinically measured end-diastolic (EDV) and end-systolic (ESV) left ventricle volumes for all identified segments over all pigs (solid line, marker circle). The crosses represent the CVS model simulation output when re-run for the identified model parameters. As can be seen the model output values match the true clinical values very well with mean absolute percentage errors less than 3 %. Figure 5 shows the same results for the right ventricle volumes, respectively.

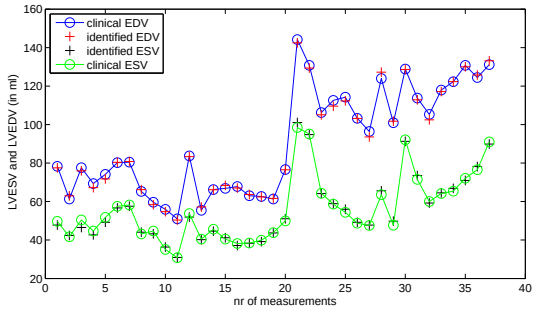

Fig. 4. Model output (cross) vs clinical (circle, solid line) left ventricle volumes for all identified segments over all pigs. The upper line shows the clinical vs. identified end-diastolic volume (LVEDV) and the lower line shows clinical vs. identified end-systolic volume (LVESV).

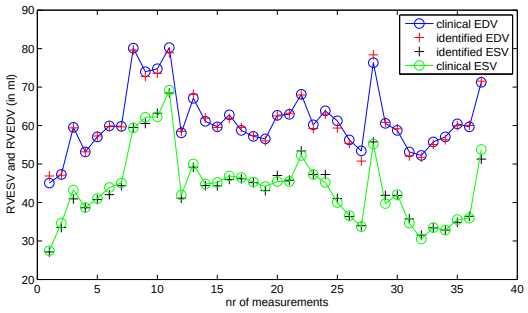

Fig. 5. Model output (cross) vs clinical (circle, solid line) right ventricle volumes for all identified segments over all pigs. The upper line shows the clinical vs. identified end-diastolic volume (RVEDV) and the lower line shows clinical vs. identified end-systolic volume (RVESV).

Figure 6 plots the matched systemic arterial systolic and diastolic pressure values (SAP, DAP) where the solid line (with circles) represents the clinical measurement and the crosses the CVS model output. Again, excellent matches are obtained with mean absolute percentage errors less than 8 %. Figure 7 has the same results for the systolic and diastolic pulmonary artery pressures (SPAP, DPAP), respectively. Note, that the match between the two signals shows larger errors for measurements 34-38, this is because the P_{pa}- measurement went below zero, a value which is non physiological and a measurement error which is ignored during the identification process.

Figure 8 and 9 illustrate the very good matches for one pig in more detail at the beginning of the experiment (T000) and at 120 minutes into the experiment(T120). The upper panel of the left subfigure (LV) shows the clinical (V_{lvp}) vs. simulated left ventricle volume (V_{lvs}) and in the lower panel the clinical (P_{lvp}) vs. simulated left ventricle pressure (P_{lvs}) and arterial pressure (P_{aop}, P_{aos}), respectively.

Note that during the identification process only the systolic and diastolic values of the ventricle volume (EDV, ESV) and arterial pressure (SAP, DAP) are used where in this experiment the left and right ventricle pressure waveforms are also available. The left ventricle pressure (P_{lv}) is not used as this measurement is rarely obtainable in a clinical setting. However, relatively good overall matches are still obtained for the ventricle pressure, further validating the model and identification process. The ventricle pressures shapes could easily be matched more accurately by adjusting the activation functions in the CVS model, however this was not required in this study. The right subfigure (RV) illustrates the same results for the right ventricle volume (V_{rv}, upper panel) and the right ventricle pressure and pulmonary artery pressure (P_{rv}, P_{pa}, lower panel).

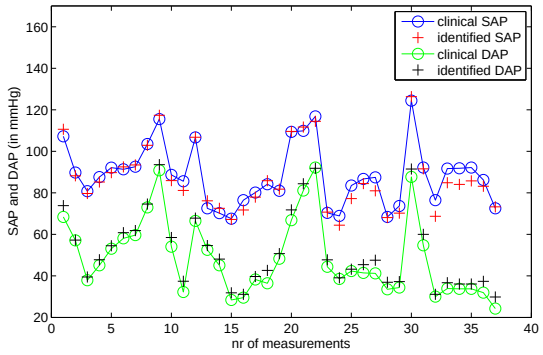

Fig. 6. Model output (cross) vs clinical (circle, solid line) arterial pressure for all identified segments over all pigs. The upper line shows the clinical vs. identified systolic arterial pressure (SAP) and the lower line shows clinical vs. identified diastolic arterial pressure (DAP).

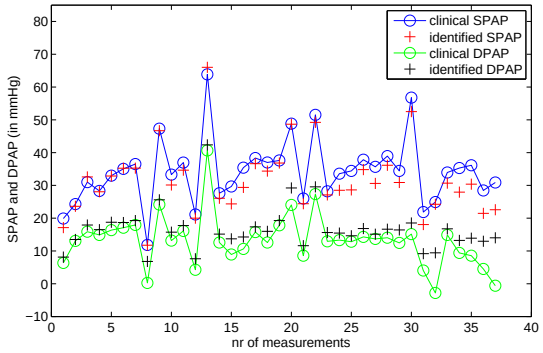

Fig. 7. Model output (cross) vs clinical (circle, solid line) pulmonary artery pressure for all identified segments over all pigs. The upper line shows the clinical vs. identified systolic pulmonary artery pressure (SPAP) and the lower line shows clinical vs. identified diastolic pulmonary artery pressure (DPAP).

Further note that, in this study it was not intended to accurately match all the details in the pressure and volume waveform shapes, but rather to identify the overall macro, hemodynamic condition. For example the dicrotic notch in the arterial pressure signals is not captured as it is not considered to be a macro driver in CVS dynamics.

Table 1 shows the mean absolute percentage errors for the identified minimum and maximum pressure and volume signals (SAP, SPAP, LVESV, LVEDV, RVEDV, RVESV)

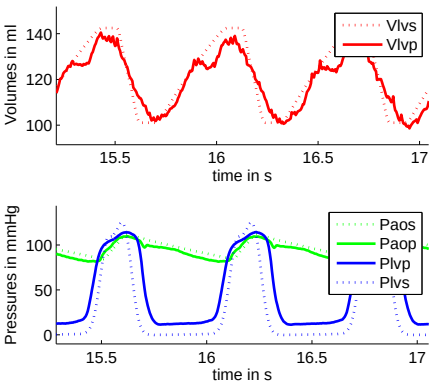

(a) time: 0 min, LV

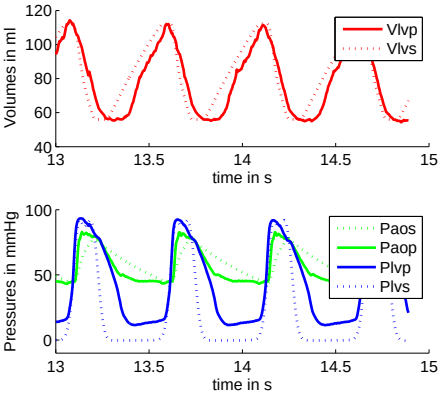

(a) time: 120 min, LV

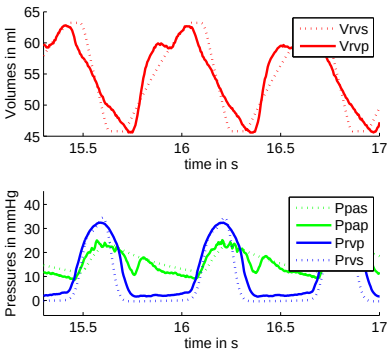

(b) time: 0 min, RV

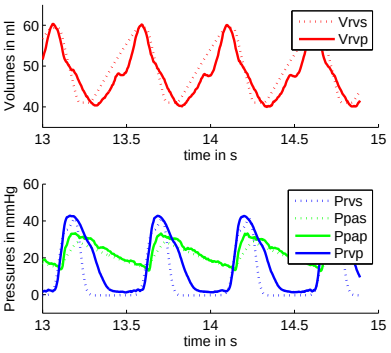

(b) time: 120 min, RV

Fig. 8. Model output (dotted) vs clinical (solid line) volume and pressure signals for left and right ventricle (LV, RV). The upper panel shows the clinical (p) vs. simulated ventricle volume (s). The lower panel shows the clinical (p) vs. simulated (s) ventricle and arterial pressure. The results are shown for T0

Fig. 9. Model output (dotted) vs clinical (solid line) volume and pressure signals for left and right ventricle (LV, RV). The upper panel shows the clinical (p) vs. simulated ventricle volume (s). The lower panel shows the clinical (p) vs. simulated (s) ventricle and arterial pressure. The results are shown for T120

Difference in % for measured and simulated pressures and volumes						
	SAP	SPAP	LVEDV	LVESV	RVEDV	RVESV
μ	3.19	8.63	1.36	2.12	1.18	1.90
σ	2.70	7.16	1.00	1.62	1.07	1.53

Table 1. Mean absolute percentage error and standard deviation in % for measured and simulated pressures and volumes over all 38 identified segments. SAP = systolic arterial pressure, SPAP = systolic pulmonary artery pressure, LVEDV = left ventricle end-diastolic volume, LVESV = left ventricle end-systolic volume, RVEDV = right ventricle end-diastolic volume, RVESV = right ventricle end-systolic volume .

over all pigs. Generally the errors are well below 10 % which is within measurement noise.

3.2 Analysis of right ventricular-vascular coupling

Figure 10 shows the RV-vascular coupling (E_{esrvf}/R_{pulin}) during the endotoxic shock experiment for two different values of V_0. To determine V_0 usually requires highly invasive measurements [Kolh et al., 2005] therefore $V_0 = 0$ is assumed for simplicity. Interestingly, the simple measured of E_{esrvf}/R_{pulin} with $V_0 = 0$ captures quite accurately both the magnitude and trend of the more sophisticated coupling measure in [Lambermont et al., 2006]. The example of $V_0 = 23$ ml is given to show that it only affects the magnitude while the trend remains similar.

4. DISCUSSION

The major findings of this research are twofold. Firstly the results that were obtained previously [Lambermont et al., 2006] are confirmed using the extended CVS model and parameter identification process. In Figure 10 it can be seen how hemofiltration (which starts at 60 min into

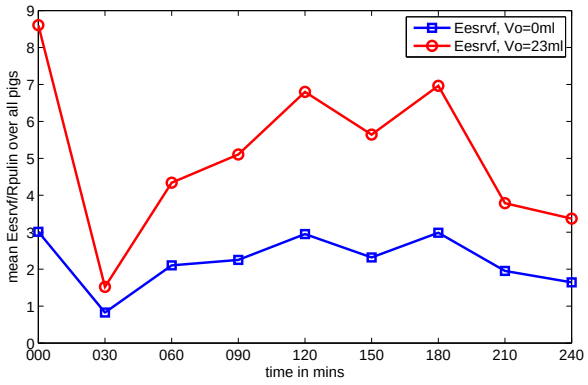

Fig. 10. Mean identified right ventricular-vascular coupling (E_{esrvf}/R_{pulin}) for all 5 analyzed pigs during the endotoxic shock experiment.

the experiment) is able to prevent RV-vascular uncoupling that is commonly observed during the late phases of endotoxic shock [Lambermont et al., 2003]. These results allow for a better understanding of the mechanisms of RV dysfunction during septic shock and thus have the potential to lead to more effective therapies of myocardial depression in septic shock.

The second key result is the further validation of the CVS model and identification process including the accurate capturing of the invasive coupling measure [Lambermont et al., 2006], the left and right ventricle pressures without measuring them and matching a significant range of hemodynamics.

These results show that the extended CVS model is able to capture the essential dynamics of the porcine CVS response to endotoxic shock and CVVH over a selection of subjects.

5. CONCLUSION

The integral-based optimization successively identified pig-specific parameters for the extended CVS model. This further validation shows the ability of the model to adequately and realistically capture the impact of pressure-volume changes during endotoxic shock and with CVVH. Comparable results to previously reported studies are obtained when analyzing the RV-vascular coupling, further validating the presented methods and approach. This research thus further confirms and increases confidence in the clinical applicability and validity of this overall model-based cardiac diagnosis and therapy approach for critical care.

REFERENCES

D. C. Angus and M. A. Crowther. Unraveling severe sepsis: why did optimist fail and what's next? *JAMA*, 290(2): 256–258, Jul 2003.

D. C. Angus, W. T. Linde-Zwirble, G. Clermont, M. F. Griffin, and R. H. Clark. Epidemiology of neonatal respiratory failure in the united states: projections from california and new york. *Am J Respir Crit Care Med*, 164(7):1154–1160, Oct 2001.

D. Chemla, J. L. Hébert, C. Coirault, K. Zamani, I. Suard, P. Colin, and Y. Lecarpentier. Total arterial compliance estimated by stroke volume-to-aortic pulse pressure ratio in humans. *Am J Physiol*, 274(2 Pt 2):500–505, Feb 1998.

D. C. Chung, S. C. Niranjan, J. W. Clark, A. Bidani, W. E. Johnston, J. B. Zwischenberger, and D. L. Traber. A dynamic model of ventricular interaction and pericardial influence. *Am J Physiol*, 272(6 Pt 2):2942–2962, Jun 1997.

C. E. Hann, J. G. Chase, J. Lin, T. Lotz, C. V. Doran, and G. M. Shaw. Integral-based parameter identification for long-term dynamic verification of a glucose-insulin system model. *Comput Methods Programs Biomed*, 77 (3):259–270, Mar 2005.

C. E. Hann, J. G. Chase, and G. M. Shaw. Integral-based identification of patient specific parameters for a minimal cardiac model. *Comput Methods Programs Biomed*, 81(2):181–192, Feb 2006.

P. Kolh, B. Lambermont, A. Ghuysen, V. Tchana-Sato, J.-M. Dogné, J. Hanson, P. Gérard, V. D'Orio, L. Piérard, and R. Limet. Effects of dobutamine on left ventriculoarterial coupling and mechanical efficiency in acutely ischemic pigs. *J Cardiovasc Pharmacol*, 45(2):144–152, Feb 2005.

B. Lambermont, A. Ghuysen, P. Kolh, V. Tchana-Sato, P. Segers, P. Gérard, P. Morimont, D. Magis, J. M. Dogné, B. Masereel, and V. D'Orio. Effects of endotoxic shock on right ventricular systolic function and mechanical efficiency. *Cardiovasc Res*, 59(2):412–418, Aug 2003.

B. Lambermont, P. Delanaye, J. M. Dogné, A. Ghuysen, N. Janssen, B. Dubois, T. Desaive, P. Kolh, V. D'Orio, and J. M. Krzesinski. Large-pore membrane hemofiltration increases cytokine clearance and improves right ventricular-vascular coupling during endotoxic shock in pigs. *Artif Organs*, 30(7):560–564, Jul 2006.

J. B. Olansen, J. W. Clark, D. Khoury, F. Ghorbel, and A. Bidani. A closed-loop model of the canine cardiovascular system that includes ventricular interaction. *Comput Biomed Res*, 33(4):260–295, Aug 2000.

B. W. Smith. *Minimal haemodynamic modelling of the heart & circulation for clinical application*. PhD thesis, University of Canterbury, 2004.

C. Starfinger, C. E. Hann, J. G. Chase, T. Desaive, A. Ghuysen, and G. M. Shaw. Model-based cardiac diagnosis of pulmonary embolism. *Comput Methods Programs Biomed*, 87(1):46–60, Jul 2007.

Y. Zhu, J. Dai, and J.K.-J. Li. Total systemic arterial compliance: evaluation of time and frequency domain methods. *Bioengineering Conference, Proceedings of the 1995 IEEE 21 Annual Northeast*, 1995.